Meng GAO, Yue-hong SHEN, Kui XU

Institute of Communications Engineering, PLA University of Science and Technology

A low complexity frequency domain pilot time domain doubly-average channel estimation for LOFDM systems

Abstract. *In this work, a low complexity time domain channel estimation algorithm for LOFDM (Lattice Orthogonal Frequency Division Multiplexing) systems is proposed through doubly-average based on the equivalent time-frequency subspace projection and traditional frequency domain pilot time domain average (FPTA) algorithm with special pilot design. Furthermore, the interference problem is analyzed and the Cramér-Rao bound (CRB) of the time domain channel estimation for LOFDM systems is also deduced. Our theoretic analyses are confirmed by numerical results.*

Streszczenie. *Zaproponowano algorytm określania w dziedzinie czasu kanałów dla systemu LOFDM bazujący na projekcji czasowo-częstotliwościowej podprzestrzeni oraz systemu pilota FPTA. Przeanalizowano problem zakłóceń. Analizę teoretyczną potwierdziły rezultaty numeryczne. (**Określanie kanałów w systemie LOFDM metodą algorytmu FPTA**)*

Keywords: LOFDM; time-frequency subspace projection; channel estimation; Cramér-Rao bound.
Słowa kluczowe: LOFDM, określanie kanałów.

Introduction

LOFDM (Lattice Orthogonal Frequency Division Multiplexing), which is proposed by Strohmer T and Beaver S in 2003 [1], has higher spectral efficiency and better bit error rate (BER) performance compared with OFDM systems in the doubly dispersive channel. To minimize the joint inter-symbol interference (ISI) and inter-carrier interference (ICI) caused by the doubly dispersive channel, the LOFDM systems use the pulse shape with optimal time-frequency (TF) concentration as the transmission pulse and design time-frequency lattice (TFL) based on the Sphere Packing theory. Until now, researches on the LOFDM systems focus on the adaptation of TFL [2], design of pulse shape [1][3], synchronization and fast modulation-demodulation [4][5].

LOFDM systems need to adapt the parameters of signals' TFL and shaping-pulse scale to the channel dispersion characteristics in the transmitters, while the exact channel impulse response (CIR) estimation is also very important to the coherent demodulation. On the other hand, in the fast varying channel environments, LOFDM signal's no CP (Cyclic Prefix) structure decides that the channel estimation can not ignore the influence of ISI/ICI interferences [6]-[9]. Since the ISI/ICI interferences destroy the integrality of data, the frequency domain channel estimation is difficult to realize [10], which is also disadvantageous for the realization of a joint interference cancellation algorithm. In conclusion, the time domain channel estimation is very attractive to the LOFDM systems.

However, the data symbols of LOFDM signal are transmitted at nonrectangular lattice point of TF plane and subcarriers are interleaved in the TF space. Because of these, we can't achieve the time domain channel estimation via the received signal directly. That is to say, the traditional OFDM channel estimation algorithm does not apply to the LOFDM systems. In this paper, based on the properties of LOFDM signals, a frequency domain pilot time domain doubly-average channel estimation algorithm is proposed. The characteristics of this algorithm are described as: firstly, separate the odd and even subcarriers of LOFDM signals through the equivalent time-frequency subspace projection based once average; secondly, a low complexity time domain channel estimation algorithm for LOFDM systems is proposed on the base of pilot design and traditional frequency domain pilot time domain average method over frequency-selective block-fading channels. The interference problem is analyzed and the Cramér-Rao bound (CRB) of the time domain channel estimation for LOFDM systems is also deduced.

The rest of this paper is organized as follows. In section II, we briefly review the basic structure of LOFDM systems. In the next section, the FPTDA algorithm is carried out. The systems performance analysis and the Cramér-Rao bound are then presented in section IV. The numerical results are provided in section VI. At the end of the paper, the remarkable conclusions are presented.

LOFDM System Model

The discrete-time LOFDM system block diagram and the TF representation of LOFDM signal are shown as Fig.1 and Fig.2, respectively. According to Fig.1 and Fig.2, the data symbol $d_{m,k}$ is pulse-shaped by $\varphi_{m,k}$, while odd and even subcarriers are interlaced with half of the symbol length to transmit over the channel. In the receiver, the conjugate function $\varphi^*_{m,k}$ of pulse-shaping function $\varphi_{m,k}$ is used to realize matched filtering demodulation, where the $\{\varphi_{m,k}\}$ is generated from the prototype pulse-shaping function φ via time-shift and frequency-modulation, and it can be expressed as

$$\begin{cases}\varphi_{m,2k}(n)=\varphi(n-m\Delta M)e^{j2\pi n2k/N}\\ \varphi_{m,2k+1}(n)=\varphi(n-m\Delta M-\Delta M/2)e^{j2\pi n(2k+1)/N}\end{cases} \tag{1}$$

where $\varphi_{m,k}$ denotes the pulse-shaping function of m-th symbol and k-th subcarrier,N is the number of the LOFDM subcarriers, ΔM denotes the length of the symbol, T_s is the sample period. Consequently, the discrete-time LOFDM signal can be expressed as [3]

$$\begin{aligned}s(n)=&\sum_{m=-\infty}^{\infty}\left[\left(\sum_{k=0}^{N/2-1}d_{m,2k}\exp(j2\pi n2k/N)\right)\varphi(n-m\Delta M)\right]\\&+\sum_{m=-\infty}^{\infty}\left[\left(\sum_{k=0}^{N/2-1}d_{m,2k+1}\exp(j2\pi n(2k+1)/N)\right)\varphi(n-m\Delta M-\Delta M/2)\right]\end{aligned} \tag{2}$$

where $d_{m,k}$ is the transmitted data m-th symbol and k-th subcarrier, $\rho=N/\Delta M$ is the spectral efficiency, the length of pulse-shaping function $\varphi=[\varphi(0),\ \varphi(1),\ldots,\ \varphi(L_\varphi\text{-}1)]$ is L_φ ($L_\varphi>\Delta M$). The base-band expression of the received signal is [5]

$$r(n)=\sum_{l=0}^{L-1}h(l,n)s(n-\tilde{\tau}_l)+w(n) \tag{3}$$

where w(n) represents the additive white Gaussian noise (AWGN), L is maximum length of channel, the discrete-time complex channel response $h(n,\tau)$ can be described by

$$h(n,\tau)=\sum_{l=0}^{L-1}h(l,n)\delta(\tau-\tilde{\tau}_l) \tag{4}$$

where $\tilde{\tau}_l$ is the delay of the l-th path, normalized by the sample period T_s, and $\tilde{\tau}_0=0$; $h(l,n)$ is the corresponding complex amplitude. Due to the motion of users, $h(l,n)$'s are wide-sense stationary (WSS) narrowband complex Gaussian

processes, and uncorrelated with each other based on the assumption of uncorrelated scattering.

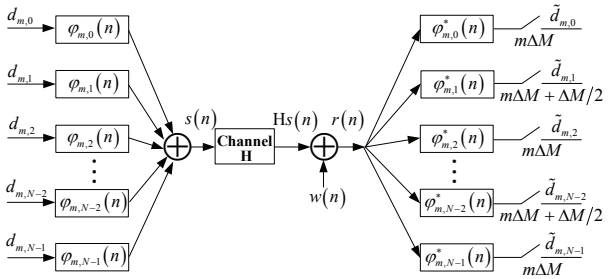

Fig.1. The discrete-time LOFDM system model

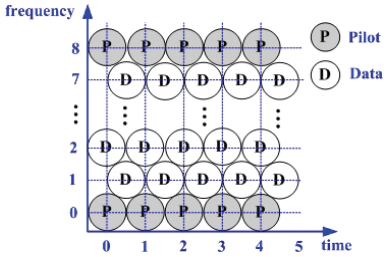

Fig.2. The TF representation of pilot-aided LOFDM systems

On the assumption of frequency-selective block-fading channel, whose pulse-shaping duration L_φ is subject to independent fading realizations, a block of signals are affected by the same fading realization. If the channel coherence time is longer than the transmission duration of each block L_φ, the channel is reasonably assumed to be constant [17][18]. The received signal vectors of the m-th symbol and length of L_φ is [6][7]

$$\begin{aligned} r_m(n) &= r_{m|m}(n) + r_{m|m-1}(n) + w_m(n) \\ &= \sum_{l=0}^{L-1} h_m(l,n)\, s_m\left(n-\tilde{\tau}_l\right)_{(L_\varphi)} \\ &\quad - \sum_{l=0}^{L-1} h_m(l,n)\, s_m\left(n-\tilde{\tau}_l\right)_{(L_\varphi)} \left(1-u\left(n-\tilde{\tau}_l\right)\right) \\ &\quad + \sum_{l=1}^{L-1} h_{m-1}(l,n)\, s_{m-1}\left(\left(n-\tilde{\tau}_l\right)_{(L_\varphi)}\right)\left(1-u\left(n-\tilde{\tau}_l\right)\right) + w_m(n) \end{aligned} \tag{5}$$

where $r_m(n)$ represents the n-th sample of the m-th LOFDM received symbol, $r_{m|m}$ is the received sample component with contributions only from block m, $r_{m|m-1}$ is the received sample component with contributions only from block m-1, $h_m(l,n)$ denotes the time-variant channel impulse response of the l-th path and $(m\Delta M+n)$-th sample, $u(n)$ is the unit step function.

FPTDA channel estimation

The data symbols of LOFDM signal are transmitted at nonrectangular lattice point of TF plane and subcarriers are interleaved in the TF space. Consequently, the dominant issue of LOFDM channel estimation is the separation of subcarriers. Considering matched filtering demodulation based separation (as Fig.1 shown), it isn't feasible in the practice due to its high computational complexity. In this section, we propose a frequency domain pilot time domain doubly-average channel estimation algorithm based on the equivalent time-frequency subspace projection to achieve the separation of carriers and estimate the CIR. And the pilot is designed to further reduce the complexity of channel estimation.

Equivalent Time-Frequency Subspace Projection

Conclusion3-1: $\boldsymbol{r}=[r(0), r(1), \ldots, r(L_\varphi\text{-}1)]$ is the received signal vector of length L_φ, $\boldsymbol{\Phi}=\{\varphi_i\}$, i=0,1, …,N/2-1 are the TF subspace sets, where $\varphi_i=\{\varphi_i(0), \varphi_i(1), \ldots, \varphi_i(L_\varphi\text{-}1)\}$, and satisfies that

$$\langle \varphi_i, \varphi_{i'} \rangle = \begin{cases} 1, & i = i' \\ 0, & i \neq i' \end{cases} \tag{6}$$

$$\varphi_i(n) = \varphi_{i'}(n) \cdot e^{j2\pi n(i'-i)/(N/2)} \tag{7}$$

Thereby, the received signal of TF subspace projection on $\boldsymbol{\Phi}$ is equivalent to the fast Fourier transform (FFT) of Hadamard product of the received signal $\boldsymbol{r}$ and φ^*_0 overlapped at the period N/2. (Proof can be seen in Appendix A)

From [16] we can know that the odd and even subcarriers can be effectively separated with the TF subspace projection. According to conclusion 3-1, we can get the time domain separated signals of via overlapping the Hadamard product of the received signal $\boldsymbol{r}$ and $\boldsymbol{\varphi}^*_0$ at the period N/2, which can be described as

$$y(p) = \sum_{l=0}^{Q_\varphi - 1} r_\varphi(p + lN/2) \tag{8}$$

where $Q_\varphi = \lceil L_\varphi/(N/2) \rceil$, $\lceil x \rceil$ denotes the minimum integer which is lager than x. $r_\varphi = r(n)\varphi^*(n)$, n=0,1, …, L_φ-1, expressed as $\boldsymbol{r}_\varphi = \boldsymbol{r} \odot \boldsymbol{\varphi}^*_0$, $\odot$ represents the Hadamard product.

Pilot Design

Based on the characteristics of LOFDM signals and the process of TF subspace projection, we choose the comb-type pilots and place all the pilots on the even sub carriers to simplify pilot signal's extraction. The pilot distance D_f is even, and the index of initial pilot subcarrier is 0. The number of the pilots is $M = N/D_f$, that is to say, the number of the subcarriers can divide by the number of the pilots. The pilot pattern is depicted as Fig.2. Thus, the pilot subcarriers set of the m-th LOFDM symbols can be expressed as $S_m = iD_f$, i=0,1, …,M-1, that is

$$d_{m,k} = \begin{cases} X_P(m,k_i) & k_i \in S_m \\ X_{Data}(m,k_{i'}) & k_{i'} \in D_m \end{cases}, k_i \neq k_{i'} \tag{9}$$

where $\boldsymbol{X}_p$ and $\boldsymbol{X}_{Data}$ are denoted as pilot vector and data vector, respectively, and D_m is the data subcarriers set of the m-th LOFDM symbols. Define all the pilots are identical, namely $X_p(m,k_i)=A$.

Once Average Based Carriers Separation

As pointed out above, all the pilots are distrusted at the even subcarriers, thereby only even subcarriers need projecting operation. The received signal vector $\boldsymbol{r}_{m0}=[r_{m0}(0), r_{m0}(1), \ldots, r_{m0}(L_\varphi\text{-}1)]$ of the $m_0\Delta M$-th symbol and length of L_φ is projected to TF subspaces. According to (8), we can get

$$y_{m_0}(p) = \sum_{l=0}^{Q_\varphi - 1} r_{m_0,\varphi}(p + lN/2) \tag{10}$$

If the channel coherence time $T_c > L_\varphi$, the channel is reasonably assumed to be constant in the observing intervals. Then, the CIR $h_{m_0}(l,n)$ can be written as $h_{m_0}(l)$, and on the conditions of the sample-spaced path delay, we can have (Deduction can be seen in Appendix B)

$$y_{m_0}(p) = \sum_{l=0}^{L-1} h_{m_0}(l) A^*_\varphi(l,0) \left[c\left((p-l)_{N/2}\right) + d\left((p-l)_{N/2}\right) \right] + I_{total}(p) \tag{11}$$

where $A^*_\varphi(l,0) = \sum_{n=0}^{L_\varphi - 1} \varphi\left((n-l)_{(L_\varphi)}\right)\varphi^*(n)$, $A_\varphi(\cdot,\cdot)$ is defined as the ambiguity function of supported interval (0,L_φ-1) [16]. $I_{total}(p)$ is the total interference, including ICI/ISI produced by multipath propagation and noise, which can be seen as Gauss noise according to central limit theory [17]. And

$$c(p) = \frac{2}{N} \sum_{i=0, k_i \in S^1_m}^{N/2-1} X_p(k_i) e^{j2\pi p k_i/(N/2)} = \frac{2A}{D_f} \sum_{r'=0}^{D_f/2-1} \delta(p - r'M) \tag{12}$$

(13) $$d(p)=\frac{2}{N}\sum_{i'=0,k_{i'}\in D_m^1}^{N/2-1}X_{data}(k_{i'})e^{j2\pi pk_{i'}/(N/2)}$$

where $S_m^1: k_i=k_0/2+iD_f/2$, i=0,1,…,M-1 is the pilot carriers set after once average operation and the data carriers set is D_m^1.

Twice Average Based CIR Estimation

With the help of once average based separation of carriers, the channel estimation of LOFDM systems has been transformed into that of OFDM. However, in formula (11), besides pilot's signal, the separated signal also contains data signal, which will interfere above channel estimation. Fortunately, thanks to the property of DFT, we can eliminate data signal effectively by averaging the received signal over $D_f/2$ periodic part. Without loss of generality, omitting index m, then the twice average process can be expressed as

(14) $$r_{yc}(l')=\frac{2}{D_f}\sum_{r=0}^{D_f/2-1}y(p-rM)=r_p(l')+r_d(l')+r_I(l')$$

(15) $$r_I(l')=\frac{2}{D_f}\sum_{r=0}^{D_f/2-1}I_{total}(p-rM)$$

(16)
$$\begin{aligned}r_p(l')&=\frac{2}{D_f}\sum_{r=0}^{D_f/2-1}\sum_{l=0}^{L-1}h(l)A^*_{\varphi}(l,0)c\left((rM+l'-l)_{N/2}\right)\\&=\frac{2}{D_f}\sum_{r=0}^{D_f/2-1}\sum_{l=0}^{L-1}h(l)A^*_{\varphi}(l,0)\frac{2A}{D_f}\sum_{r'=0}^{D_f/2-1}\delta\left((rM+l'-r'M-l)_{N/2}\right)\\&=\frac{2A}{D_f}\sum_{l=0}^{L-1}h(l)A^*_{\varphi}(l,0)\delta(l'-l)\end{aligned}$$

$$r_d(l')=\frac{2}{D_f}\sum_{r=0}^{D_f/2-1}\sum_{l=0}^{L-1}h(l)A^*_{\varphi}(l,0)d\left((rM+l'-l)_{N/2}\right)$$

(17)
$$\begin{aligned}&=\frac{2}{D_f}\sum_{r=0}^{D_f/2-1}\sum_{l=0}^{L-1}h(l)A^*_{\varphi}(l,0)\frac{2}{N}\sum_{k=0}^{N/2-1}X_{data}(k)e^{j2\pi(rM+l'-l)k/(N/2)}\\&=\sum_{l=0}^{L-1}h(l)A^*_{\varphi}(l,0)\frac{2}{N}\sum_{k'=0}^{M-1}X_{data}\left(k'\cdot\frac{D_f}{2}\right)e^{j2\pi(l'-l)k'\cdot\frac{D_f}{2}/(N/2)}\end{aligned}$$

With (9), we get $r_d(l')$=0. So, if L<M satisfies, the estimation of channel time impulse response can be derived as

(18) $$\hat{h}(l')=\frac{D_f}{2A\cdot A^*_{\varphi}(l',0)}\cdot r_{yc}=\sum_{l=0}^{L-1}h(l)\delta(l'-l)+\frac{D_f}{2A\cdot A^*_{\varphi}(l',0)}r_I(l')$$

Performance analysis

This section we will analyze the interference and noise of the systems, and the CRB of Mean Square Error (MSE) is also deduced. Before the analysis, two preconditions need to be added in the rest of the paper:

– The data symbol is independent and identically distributed (i.i.d) random vector with zero mean, and it is uncorrelated with pilot symbol. The power of data and pilot symbols is equivalent, viz. $\sigma_p^2=\sigma_d^2=E\left[\left|d_{m,k}\right|^2\right]$.

– The CIR $h_m(l)\in CN(0,\sigma_l^2)$, and $\sum_{l=0}^{L-1}\sigma_l^2=1$.

From the appendix B, we can get that

(19)
$$\begin{aligned}I_{total}(p)&=\frac{1}{N/2}\sum_{i=0}^{N/2-1}I(i)e^{j2\pi pi/(N/2)}\\&=\underbrace{\frac{1}{N/2}\sum_{i=0}^{N/2-1}\Gamma_3e^{j2\pi pi/(N/2)}}_{I_{ISI}}-\underbrace{\frac{1}{N/2}\sum_{i=0}^{N/2-1}\Gamma_2e^{j2\pi pi/(N/2)}}_{I_{ICI}}+\underbrace{\frac{1}{N/2}\sum_{i=0}^{N/2-1}w(i)e^{j2\pi pi/(N/2)}}_{I_w}\end{aligned}$$

Since the useful signal is independent with interference, and I_{ISI}, I_{ICI} and I_w are also independent and zero mean, the interference power is

(20) $$\sigma_I^2=E\left[\left|I_{total}(p)\right|^2\right]=\sigma_{ISI}^2+\sigma_{ICI}^2+\frac{\sigma_w^2}{N/2}$$

According to [7], when L<< L_φ, we have $\sigma_{ISI}^2\approx\sigma_{ICI}^2$. Thereby, it's easy to get that

(21) $$\sigma_{ISI}^2=\frac{2}{\Delta M}\sigma_d^2\sum_{l=1}^{L-1}\sigma_l^2\sum_{n=0}^{L_\varphi-1}\left[\left(1-u(n-l)\right)\varphi^*(n)\right]^2$$

Then, we have $I_{total}(p)\in CN(0,\sigma_I^2)$, and

(22)
$$\begin{aligned}\sigma_I^2&=E\left[\left|I_{total}(p)\right|^2\right]\approx 2E\left[I_{ISI}^2\right]+E\left[I_w^2\right]\\&=\frac{4}{\Delta M}\sigma_d^2\sum_{l=1}^{L-1}\sigma_l^2\sum_{n=0}^{L_\varphi-1}\left[\left(1-u(n-l)\right)\varphi^*(n)\right]^2+\frac{\sigma_w^2}{N/2}\end{aligned}$$

Rewrite formula (11) to matrix form as follows

(23) $$\boldsymbol{Y}=\boldsymbol{Ph}+\boldsymbol{Dh}+\boldsymbol{I}_{total}$$

where $\boldsymbol{P}_{i,j}$= $c((i-j)_{N/2})$, $\boldsymbol{D}_{i,j}$= $d((i-j)_{N/2})$, $\boldsymbol{Y}$=[y(0),y(1),…,r(N/2-1)]^T, $\boldsymbol{h}$=[h(0),h(1),…,h(L-1),0,…,0]^T, I_{total} is complex additive white Gaussian noise.

The conditional expectation and variance of $\boldsymbol{Y}$ is

(24) $$\left.\begin{aligned}\boldsymbol{u}_{\boldsymbol{Y}}(h)&=\boldsymbol{Ph}+\boldsymbol{Dh}\\\boldsymbol{C}_{\boldsymbol{YY}}(h)&=\sigma_I^2\boldsymbol{I}\end{aligned}\right\}$$

So the likehood can be expressed as [17]

(25) $$p(\boldsymbol{Y};\boldsymbol{h})=\frac{1}{2\pi\left|\boldsymbol{C}_{\boldsymbol{YY}}(h)\right|^{N/2}}\exp\left\{-\frac{(\boldsymbol{Y}-\boldsymbol{Ph}+\boldsymbol{Dh})^H\boldsymbol{C}_{\boldsymbol{YY}}^{-1}(h)(\boldsymbol{Y}-\boldsymbol{Ph}+\boldsymbol{Dh})}{2}\right\}$$

According to [19], the fisher information matrix $\boldsymbol{I}(\boldsymbol{h})_{i,j}$ can be calculated as

(26) $$\boldsymbol{I}(\boldsymbol{h})_{i,j}=2\mathrm{Re}\left[\frac{\partial\boldsymbol{u}_{\boldsymbol{Y}}^H(h)}{\partial h_i}\boldsymbol{C}_{\boldsymbol{YY}}^{-1}(h)\frac{\partial\boldsymbol{u}_{\boldsymbol{Y}}(h)}{\partial h_j}\right]+tr\left[C_{\boldsymbol{YY}}^{-1}(h)\frac{\partial C_{\boldsymbol{YY}}(h)}{\partial h_i}C_{\boldsymbol{YY}}^{-1}(h)\frac{\partial C_{\boldsymbol{YY}}(h)}{\partial h_j}\right]$$

With (25), $C_{YY}(h)$ is independent of $\boldsymbol{h}$, that is to say, $\partial C_{YY}(h)/\partial h_i$=0. Thus

(27)
$$\begin{aligned}\boldsymbol{I}(\boldsymbol{h})_{i,j}&=2\mathrm{Re}\left[\frac{\partial\boldsymbol{u}_{\boldsymbol{Y}}^H(h)}{\partial h_i}\boldsymbol{C}_{\boldsymbol{YY}}^{-1}(h)\frac{\partial\boldsymbol{u}_{\boldsymbol{Y}}(h)}{\partial h_j}\right]\\&=2\mathrm{Re}\left[\frac{\boldsymbol{P}_i^H\boldsymbol{P}_j+\boldsymbol{P}_i^H\boldsymbol{D}_j+\boldsymbol{D}_i^H\boldsymbol{P}_j+\boldsymbol{D}_i^H\boldsymbol{D}_j}{\sigma_I^2}\right]\end{aligned}$$

where $\boldsymbol{P}_i$=[$c_{N/2-i+1}$,$c_{N/2-i+2}$,…,$c_{N/2-i}$]^T and $\boldsymbol{D}_i$=[$d_{N/2-i+1}$,$d_{N/2-i+2}$,…,$d_{N/2-i}$]^T denote the i-th column of $\boldsymbol{P}$ and $\boldsymbol{D}$, respectively.

Like the deduction of (17), we can have

(28) $$\boldsymbol{I}(\boldsymbol{h})_{i,j}=\begin{cases}2\sigma_d^2/\sigma_I^2, & i=j\\0, & i\neq j\end{cases}$$

(29) $$\boldsymbol{I}(\boldsymbol{h})_{i,i}=\frac{1}{\frac{2}{\Delta M}\sum_{l=1}^{L-1}\sigma_l^2\sum_{n=0}^{L_\varphi-1}\left[\left(1-u(n-l)\right)\varphi^*(n)\right]^2+\frac{\sigma_w^2}{N\sigma_d^2}}$$

So the CRB of unbiased estimator $\hat{h}_i$ satisfies

(30) $$\mathrm{Var}\left(\hat{h}_i\right)\geq\boldsymbol{I}^{-1}(\boldsymbol{h})_{i,i}=\frac{1}{N}\left[\frac{1}{SNR}+2\rho\sum_{l=1}^{L-1}\sigma_l^2\sum_{n=0}^{L_\varphi-1}\left[\left(1-u(n-l)\right)\varphi^*(n)\right]^2\right]$$

Simulation and result

In this section, supposing the ideal synchronization, we discuss the MSE and symbol error rate (SER) performances of LOFDM system using FPTDA channel estimation algorithm, and compare the MSE performance of our algorithm with CRB. The specific simulation conditions are as follows:

– The spectral efficiency is ρ=0.8 and the sample period is T_s=2.5×10^{-6}s.The pulse-shaping function is derived from the generalized Gabor transform [3] and the length is L_φ=600. We use QPSK modulation and the modulation and demodulation are realized as [4].

– The number of the pilots is M=10, the space of the pilot subcarriers is D_f=4, and the amplitude of the pilot is A^2=2.

– The multipath channel is modeled as the frequency-selective block-fading channel, the maximum Doppler spread is f_d=100Hz, the power delay profile (PDP) for the channel is characterized by the exponential distribution $E[|h(l)|^2]=e^{-3l/L}$ and uniform distribution $E[|h(l)|^2]=1/L$. The numbers of paths are L=2,4,6, respectively.

In Fig.3 and Fig.4, when the number of the subcarriers is N=40 and the length of the symbol is ΔM=50, we compare the MSE performances of FPTDA with CRB on the condition that the number of channel taps L is different. It is easy to know that both the performances of FPTDA and CRB gradually decrease when L increases. On the other hand, comparing Fig.3 with Fig.4, we can find that when L is same, our algorithm can achieve better performance on the exponential PDP condition than uniform PDP. That is to say, the performance of channel estimation is decided by both the number of channel taps and the PDP, which is consistent with the CRB theoretical formula.

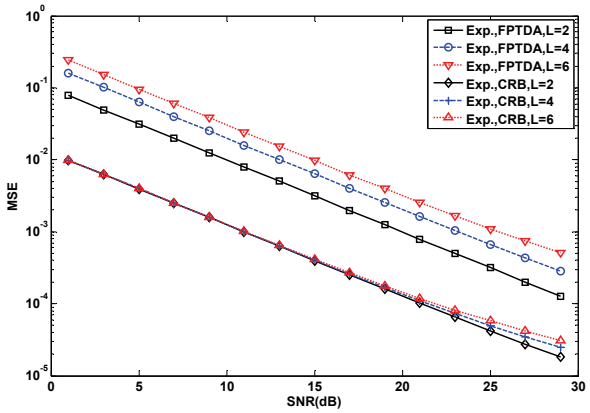

Fig.3. Exponential PDP, N=40, comparing the MSE performance of FPTDA with CRB

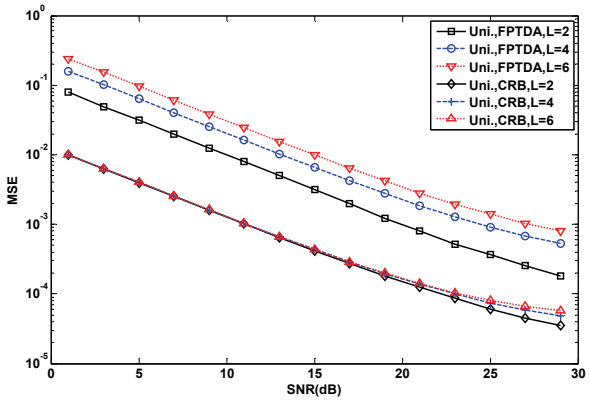

Fig.4. Uniform PDP, N=40, comparing the MSE performance of FPTDA with CRB

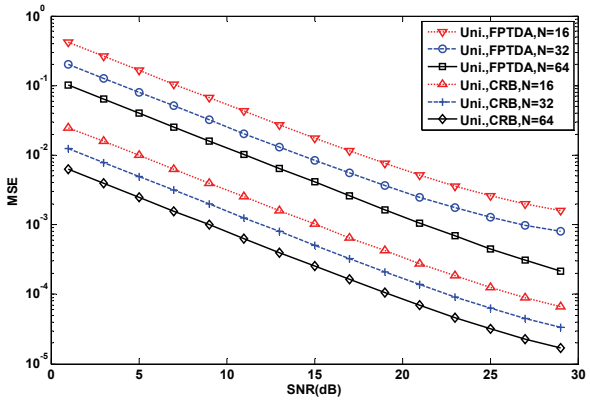

Fig.5. Uniform PDP, L=4, comparing the MSE performance of FPTDA with CRB

Fig.4 shows that the MSE performance of our algorithm appears an error floor at about 20dB when L are 4 and 6 with uniform PDP. The reason is that the number of the subcarriers N which we choose in this paper is not large, so when L increases, which is comparable with N (about $L>N/10$), the effect on the performance of the system from the interference will be stronger than the noise. From the CRB formula we know that the ability of combating the multipath interference and performance of our algorithm can be improved by adding the number of the subcarriers. Fig.5 evaluates the influence of different subcarrier numbers on the performance of FPTDA algorithm and CRB, where L=4, N=16,32,64, and the PDP of channel is characterized by uniform distribution. As seen from Fig.5, when L is fixed, the MSE performance of FPTDA can improve through increasing N, which can also solve the error floor problem to a certain extent. However, the improvement is at the cost of increasing complexity of receiver. In practice, a counterbalance is needed between power complexity and performance.

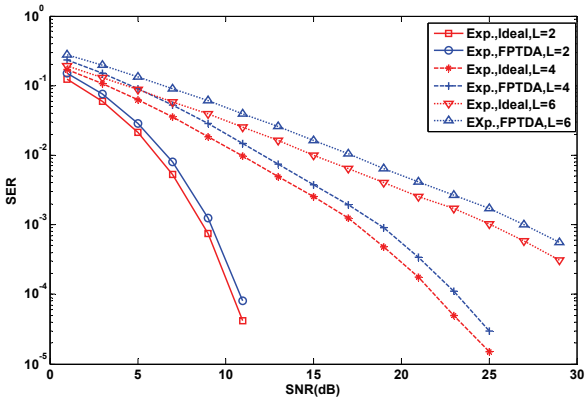

Fig.6. The SER performances of the system with exponential PDP and N=40

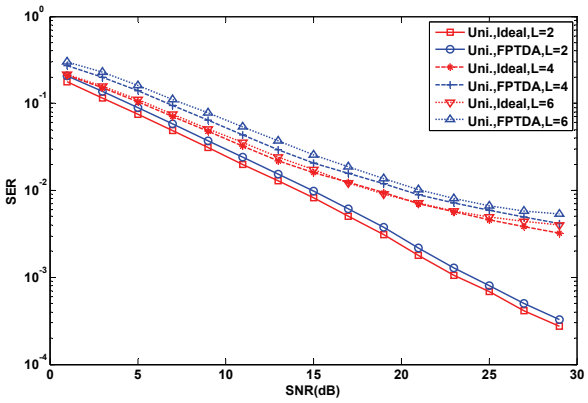

Fig.7. The SER performances of the system with uniform PDP and N=40

In Fig.6 and Fig.7, where N=40, ΔM=50, channels with exponential and uniform PDP, we depict the SER performances of the system with different multipath numbers, which uses FPTDA channel estimation value and ideal channel value to demodulate, respectively. Obviously, when L increases, the error of FPTDA channel estimation and the interference of multipaths both increase, so the SER of the system increases. It is also seen that when we use the FPTDA channel estimation value to do the demodulation, the SER performance of the system is close to that of the system when using the ideal channel value. That is to say, our algorithm has good practicability. Moreover, when the number of channel taps increases, the effect on the performance of the system from the error of channel estimation decreases gradually, and the SER performance of the system mostly depends on the interference and noise.

Complexity analysis

From above analysis we can know that, the calculating complexity of our proposed channel estimation algorithm

mainly comes from the doubly-average operation. Since, the complex addition contributes little influence to the calculating complexity, we focus on the number of complex multiplication. Once of the subspace projection based average needs $L_\varphi \times N/2$ times of multiplication, while the twice time average in the receiver needs M times of multiplication.Thereby, the calculating complexity of our algorithm is $L_\varphi \times N/2+M$ times of multiplication, viz. $O(N^2)$. The calculating complexity of our algorithm is low.

Conclusion

In this paper, based on the characteristics of LOFDM systems and equivalent TF subspace projection, a low complexity LOFDM time-domain doubly-average channel estimation algorithm is proposed in the frequency-selective block-fading channels. Theory analyses and simulations demonstrate that on the different channel conditions the proposed algorithm has good MSE performance between the estimated CIR and the true CIR, while SER performance of demodulation through the estimated CIR is near with the ideal channel. Furthermore, the interference problem is analyzed and the Cramér-Rao bound (CRB) of the time domain channel estimation for LOFDM systems is also deduced.

This work is supported by the National Natural Science Foundation of China under Grant 60772083.

Appendix A

Proof: the data symbol projected to the i-th TF subspace is

$$Y(i)=\langle r,\varphi_i\rangle=\sum_{n=0}^{L_\varphi-1} r(n)\varphi_i^*(n)=\sum_{n=0}^{L_\varphi-1} r(n)\varphi_0^*(n)e^{-j2\pi ni/(N/2)} \tag{A1}$$

Taking $N/2$-point IFFT on the projecting signal of TF subspace set $\boldsymbol{\Phi}$, we have

$$\begin{aligned} y(p)&=\frac{1}{N/2}\sum_{i=0}^{N/2-1} Y(i)e^{j2\pi pi/(N/2)}\\ &=\frac{1}{N/2}\sum_{i=0}^{N/2-1}\sum_{n=0}^{L_\varphi-1} r(n)\varphi_0^*(n)e^{-j2\pi ni/(N/2)}e^{j2\pi pi/(N/2)}\\ &=\frac{1}{N/2}\sum_{i=0}^{N/2-1}\sum_{n=0}^{L_\varphi-1} r(n)\varphi_0^*(n)e^{j2\pi(p-n)i/(N/2)}\\ &=\frac{1}{N/2}\sum_{i=0}^{N/2-1}\sum_{n=0}^{N/2-1}\sum_{l=0}^{Q_\varphi-1} r_\varphi(n+lN/2)e^{j2\pi(p-n)i/(N/2)}\\ &\underset{k=n}{=}\sum_{l=0}^{Q_\varphi-1} r_\varphi(n+lN/2) \end{aligned} \tag{A2}$$

Appendix B

$$\begin{aligned} Y_{m_0}(i)&=\sum_{n=0}^{L_\varphi-1} r_{m_0}(n)\varphi_i^{1*}(n)\\ &=\sum_{n=0}^{L_\varphi-1} r_{m_0|m_0}(n)\varphi_i^{1*}(n)+\sum_{n=0}^{L_\varphi-1} r_{m_0|m_0-1}(n)\varphi_i^{1*}(n)+\sum_{n=0}^{L_\varphi-1} w_{m_0}(n)\varphi_i^{1*}(n)\\ &=d_{m_0,2i}\sum_{n=0}^{L_\varphi-1}\sum_{l=0}^{L-1} h_{m_0}(l)e^{-j2\pi li/(N/2)}\varphi\left((n-l)_{(L_\varphi)}\right)\varphi^*(n)\\ &\quad-\underbrace{\sum_{n=0}^{L_\varphi-1}\left[\sum_{l=0}^{L-1} h_{m_0}(l)s_{m_0}\left((n-l)_{(L_\varphi)}\right)\left(1-u(n-l)\right)\right]\varphi_i^{1*}(n)}_{\tilde{\Gamma}_2}\\ &\quad+\underbrace{\sum_{n=0}^{L_\varphi-1}\left[\sum_{l=0}^{L-1} h_{m_0-1}(l)s_{m_0-1}\left((n-l)_{(L_\varphi)}\right)\left(1-u(n-l)\right)\right]\varphi_i^{1*}(n)}_{\tilde{\Gamma}_3}+w(i) \end{aligned} \tag{B1}$$

where the first, second and third item are the useful signal, the ICI/ISI interference and noise, respectively, $(\cdot)_N$ denotes the module N procession. Since the linear transformation of Gauss random vectors also follows Gauss distribution, we can get that $w(i)=\sum_{n=0}^{L_\varphi-1} w_{m_0}(n)\varphi_i^{1*}(n)$ is a Gauss random vector, and $w(i)\in CN(0,\sigma_w^2)$. The above formula can be simply expressed as

$$Y_{m_0}(i)=d_{m_0,2i}\sum_{l=0}^{L-1} A_\varphi^*(l,0)h_{m_0}(l)e^{-j2\pi li/(N/2)}+I_{total}(i) \tag{B2}$$

where $I_{total}(i)=\tilde{\Gamma}_3-\tilde{\Gamma}_2+w(i)$, according to central limit theory [13], $I_{total}(i)$can be seen as Gauss noise. After theTF subspace projection, the pilot carriers set can be written as $S_m^1: k_i=k_0/2+iD_f/2$, i=0,1,…,M-1, the data carriers set is D_m^1, taking IFFT on the both sides of the formula (B.2), we have (see (B3) at the bottom)

$$\begin{aligned} y(p)&=\frac{1}{N/2}\sum_{i=0}^{N/2-1} d_{m_0,2i}\sum_{l=0}^{L-1}\sum_{n=0}^{L_\varphi-1} A_\varphi^*(l,0)h_{m_0}(l)e^{-j2\pi li/(N/2)}e^{j2\pi pi/(N/2)}+\frac{1}{N/2}\sum_{i=0}^{N/2-1} I_{total}(i)e^{j2\pi pi/(N/2)}\\ &=\sum_{l=0}^{L-1} h_{m_0}(l)A_\varphi^*(l,0)\frac{2}{N}\left[\sum_{i=0,k_i\in S_m^1}^{N/2-1} X_p(k_i)e^{j2\pi(p-l)k_i/(N/2)}+\sum_{i'=0,k_{i'}\in D_m^1}^{N/2-1} X_{data}(k_{i'})e^{j2\pi(p-l)k_{i'}/(N/2)}\right]+I_{total}(p)\\ &=\sum_{l=0}^{L-1} h_{m_0}(l)A_\varphi^*(l,0)\frac{2}{N}\left[c(p-l)+d(p-l)\right]+I_{total}(p) \end{aligned} \tag{B3}$$

REFERENCES

[1] Strohmer T, Beaver S., Optimal OFDM design for time–frequency dispersive channels, IEEE Trans. on Commun., 51(2003), No.7, 1111-1122

[2] Z. G. Yuan and Y. H. Shen, A novel LOFDM signal and its optimization over doubly-dispersion channels, ICIEA, Singapore, 2008

[3] Jian Wei, Shen Y.H. and Li Yi, Pulse-shaping based on general gabor transform for optimal LOFDM system, Journal of Electronics & Information Technology, China, 28(2006), No.7, 1274-1278

[4] Jian Wei, Research of performance analysis and application for LOFDM systems, Ph.D. dissertation, PLA University of Science and Technology, China, Jun. 2006.

[5] Xu Kui, Shen Yue-hong, Chen Shou-qi, Blind Estimation of Large Carrier Frequency Offset in LOFDM Systems, Signal Processing, China, 25(2009), No.10, 1537-1541

[6] Xianbin Wang, Paul Ho, and Yiyan Wu, Robust channel estimation and ISI cancellation for OFDM systems with suppressed features, IEEE J. Sel. Area Commun., 23(2005), No.5, 963-972

[7] Dukhyun Kim, and Gordon L. St¨uber, Residual ISI cancellation for OFDM with applications to HDTV broadcasting, IEEE J. Sel. Area Commun., 16(1998), No.8, 1590-1599

[8] Wei Zhong, Zhigang Mao, Efficient Time-Domain Residual ISI Cancellation for OFDM-Based WLAN Systems, IEEE Transactions on Consumer Electronics, 52(2006), No.2, 321-326

[9] Shaoping Chen, Cuitao Zhu, ICI and ISI Analysis and Mitigation for OFDM Systems with Insufficient Cyclic Prefix in Time-Varying Channels, IEEE Transactions on Consumer Electronics, 50(2004), No.1, 78-83

[10] Tirnner Y. and Bergenlid M., Estimating the Ineter Cell Dependency Matrix in a GSM network, IEEE VTC 0-7803-5435-4, 1999, 3024-3028

[11] X. Wang, Y. Wu, J. Y. Chouinard, S. Lu, and B. Caron, A channel characterization technique using frequency domain pilot time domain correlation method for DVB-T systems, IEEE Trans. Consumer Electronics, 50(2004), No.4, 1049-1057

[12] C. S. Yeh and Y. Lin, Channel estimation using pilot tones in OFDM systems, IEEE Trans. Broadcasting, 45(1999), No.4, 400–409

[13] M. Li, J. Tan, and W. Zhang, A channel estimation method based on frequency-domain pilots and time-domain processing for OFDM systems, IEEE Trans. Consumer Electronics, 50(2004), No.4, 1049-1057

[14] H. Minn and V. K. Bhargava, An investigation into time-domain approach for OFDM channel estimation, IEEE Trans. Broadcasting, 2000, 46(4): 240–248

[15] Bowei Song, Lin Gui, and Wenjun Zhang, Comb type pilot aided channel estimation in OFDM systems with transmit diversity, IEEE Trans. on Broadcasting, 2006, 52(1):50-57

[16] Zhang Xian-da, Bao Zheng, Nonstationary signal analysis and processing, National Defense Industry Press, Beijing, China, 1998

[17] J. G. Proakis. Digital Communications, 5th Ed, New York: McGraw-Hill, Jun., 2009

[18] P. A. Bello, Characterization of randomly time-variant linear channels, IEEE Trans. Commun. Syst., 11(1963), 360–393

[19] S. M. Kay, Fundamentals of Statiscial Signal Processing, vol.1: Estimation Theory, Prentice, Hall PTR, 1993

***Authors**: Dr. Meng Gao, Wireless Communication Faculty, Institute of Communications Engineering, E-mail: gaomeng0323@163.com; Prof. Yue-hong Shen, Wireless Communication Faculty, Institute of Communications Engineering, E-mail: chunfeng22259@126.com; Dr. Ku Xu, Wireless Communication Faculty, Institute of Communications Engineering, E-mail: xiancheng_2005@163.com.*